JOURNAL OF GEOPHYSICAL RESEARCH, VOL. 95, NO. C8, PAGES 12,995–13,008, AUGUST 15, 1990

The Flow of the Undercurrent Over the Continental Borderland off Southern California

RONALD J. LYNN

Southwest Fisheries Center, National Marine Fisheries Service, National Oceanic and Atmospheric Administration, La Jolla, California

JAMES J. SIMPSON

Scripps Institution of Oceanography, La Jolla, California

Complex bathymetric features offshore of southern California have a pronounced effect upon the flow of the California Undercurrent. Geostrophic dynamics and water mass characteristics are used to reveal the various paths of flow and spread of undercurrent waters for a July 1985 survey. Undercurrent waters are identified by relatively high spiciness and low dissolved oxygen at densities between σ_t = 26.4 and 26.9 (~200 to 400 m). A jetlike core of flow follows the continental slope within the California Bight and exits the bight through a gap in the Santa Rosa–Cortes Ridge. Mixtures that include undercurrent waters exit the bight through other gaps in the bathymetric ridge and about the southern end of the ridge. As evidenced by patterns in the fields of geostrophic currents and water mass characteristics, baroclinic instabilities develop about the ridge which result in the diversion of undercurrent waters offshore beneath the California Current and into the offshore mesoscale eddy field. The offshore subsurface diversion of undercurrent waters and their inclusion in the offshore mesoscale eddy field are also found in the long-term mean distributions for July.

1. INTRODUCTION

The bottom topography off southern California has been termed a continental borderland to distinguish it from the ordinary shelf-slope morphology found along most continental margins [*Shepard and Emery*, 1941]. Islands, shallow banks, basins, and troughs form a complex bathymetric region extending from the coast to 200 km offshore. The southern California coastline has a concave curvature between the headland at Point Conception to the U.S.–Mexican border. As a whole, this region is referred to as the California Bight. The geographic–bathymetric configuration of the bight exerts a pronounced influence upon the local circulation patterns and hence upon the distributions of physical [e.g., *Sverdrup and Fleming*, 1941] and biological quantities [e.g., *Allen*, 1945; *Owen*, 1980]. During 1985 we conducted an oceanographic survey off southern California. The sampling grid was designed to reveal the influence of the geographic–bathymetric features upon the circulation of the California Current system (CCS), especially the flow of the California Undercurrent (CU). The survey grid also includes station lines across the core of the California Current (CC) and transects an offshore dipole eddy [*Simpson and Lynn*, this issue]. The station grid of this study differs considerably from that used by the California Cooperative Oceanic Fisheries Investigations (CalCOFI) surveys in both its spatial resolution and depth of sampling. The objectives of this report are (1) to examine the spatial continuity of the CU through the complex bathymetry of the bight, (2) to trace the poleward paths and offshore spread of waters of southern origin transported by the CU, (3) to contrast this subsurface flow with the surface flow, and (4) to compare these results with the long-term CalCOFI mean conditions.

Paper number 89JC03291.
0148-0227/90/89JC-03291$05.00

2. BACKGROUND

The CC, a slow, broad equatorward flow, is the eastern limb of the large-scale anticyclonic gyre of the temperate North Pacific Ocean. The CC carries relatively cool, low-salinity waters of subarctic origin to lower latitudes. On average, the core of the CC has velocities of 0.10 to 0.15 m s^{-1} and traces a path roughly parallel to the California–Baja California coastline. Localized measurements of flow can exceed 0.5 m s^{-1} [*Davis*, 1985]. An instantaneous realization of the CC includes a tangle of meanders, eddies, and narrow jetlike flows and counterflows. The CC lies at varying distances off the coast, and at the latitude of the U.S.–Mexican border there is a strong shoreward component to the flow. In most seasons (especially summer) the flow splits; one branch turns and flows northward into the California Bight, becoming the eastern limb of a cyclonic eddy centered about the offshore banks. Seasonally (fall and winter) a weak Inshore Countercurrent (IC) develops at the surface along various portions of the coastline [*Reid et al.*, 1958]. At depth the CU carries waters of subtropical origin poleward along the continental slope. These waters are relatively warm and saline and have low concentrations of dissolved oxygen. The CU also demonstrates a well-defined seasonality and at times opposes the overlying surface flow. Maps and sections of the long-term seasonal means of relative geostrophic velocity and distributions of ocean characteristics for the CCS are available in CalCOFI Atlas 30 [*Lynn et al.*, 1982]. For a comprehensive review of the long-term seasonal, large-scale description of the CCS, the reader is referred to recent papers by *Hickey* [1979], *Chelton* [1984], and *Lynn and Simpson* [1987] and to important references of pioneering work given therein.

The waters of the bight were first studied in detail by *Sverdrup and Fleming* [1941], who presented a very perceptive study based on a series of three cruises conducted in the spring and summer of 1937. They identified a shallow poleward flow (that they termed the Southern California Counter Current) as part of a large cyclonic eddy. They recognized that this current is different from a deep poleward current (the CU) which carries characteristically

different water. They suggested that the topography of the bottom plays a large part in determining the character of the currents, especially the subsurface currents. In an examination of the different water masses, they identified waters of northern and southern origins and showed that part of the southern water flows through the deeper gaps in the submerged ridge that projects south-southeast from Santa Rosa Island. From there the flow continues north. They also argued that large-scale mixing must take place between the CC and the countercurrents. They hypothesized that the mixing is brought about by eddies because their data showed that patches of water, of mostly southern origin, were surrounded by water of mostly northern origin.

Direct measurements of the CU off central California were made by *Reid* [1962] using drifters tethered to drogues at 250 m. He found speeds of 0.23 m s^{-1} within 74 km of the coast. Using a profiling current meter, *Wooster and Jones* [1970] showed that the CU off Punta Colnett, northern Baja California, can manifest itself as a narrow (20 km) ribbon of flow having an average speed of 0.3 m s^{-1}. The seasonal variation of the geostrophic velocity and associated characteristics of temperature, salinity, and dissolved oxygen at levels of the CU were described for the cardinal CalCOFI station lines, from central California to southern Baja California, by *Lynn and Simpson* [1987]. CalCOFI line 90 bisects the California Bight and provides the long-term seasonal means for this study. The extensive CalCOFI data are most useful for examining mesoscale to large-scale processes but lacks the spatial resolution necessary to examine bathymetric interactions with the flow of the CU in the bight, especially its continuity and path.

3. THE OBSERVATIONS

The station positions for the RV *David Starr Jordan* survey of July 11–27, 1985, are given in Figure 1. Principal landmarks are identified in the caption. Within the California Bight, station lines are perpendicular to the local continental slope; they cross channels and basins between islands, banks, and the mainland. West and southwest of the bight the station lines lie perpendicular to the path of the CC as given by the long-term July mean pattern of dynamic height [*Lynn and Simpson*, 1987]. The double cross of stations west of 122°W overlays an eddy dipole observed in satellite surface temperature patterns for July 9, 1985 [*Simpson and Lynn*, this issue]. Most of the spacing between stations varies between 12 and 22 km; it is less than 12 km where it was necessary to accommodate narrow channels. Where bottom depth permitted, conductivity-temperature-depth-oxygen (CTDO2) (Neil Brown Inc. Mark III) casts were made to 1000 m (1200 m in the eddy dipole). Within the bight, where bottom depth is mostly less than 1000 m, station transects begin and end at the 500-m isobath. All eight stations in the Santa Barbara Channel are less than 500 m, as are several stations near the outer banks.

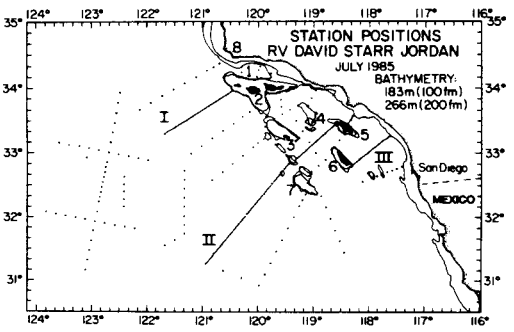

Fig. 1. Station positions of RV *David Starr Jordan* cruise, July 1985. Numbers identify the following features: 1, Santa Barbara Channel; 2, Channel Islands (San Miguel, Santa Rosa, Santa Cruz, and Anacapa); 3, San Nicolas Island; 4, Santa Barbara Island; 5, Santa Catalina Island; 6, San Clemente Island; 7, Tanner and Cortes banks; and 8, Pt. Conception. Roman numerals identify station lines used in subsequent figures.

Beam transmission was measured at 660 nm using a beam transmissometer with a 25-cm path length (Sea Tech, Inc.) attached to the CTD. Beam transmission is a good indicator of concentration of suspended matter and is used to differentiate near coastal water, having suspensoids of plankton and terrigenous materials, from the more sterile oceanic waters. A 12-bottle rosette was used to obtain temperature, salinity, and oxygen calibration measurements for the CTDO2. Dissolved oxygen titration check samples were taken every fourth station or so, 43 stations in all. Twelve samples per cast were taken on 13 stations, and four or five samples were taken on the remaining 30 stations. Oxygen probe measurements were processed using an experimental algorithm developed with the assistance of the Physical and Chemical Oceanographic Data Facility at Scripps Institution of Oceanography (SIO). A single set of coefficients was applied to all casts that reduced the standard deviation between check samples and probe data to less than ±0.1 mL L^{-1}. Long-term experience has shown us that considerable problems can arise in the use of this style oxygen probe. This particular data set, on the whole, lacked serious problems and its application and interpretation herein is based on values of oxygen concentration and its gradients that greatly exceed any reasonable estimate of measurement or calibration error.

4. BATHYMETRY AND ITS EFFECT ON THE CALCULATION OF DYNAMIC HEIGHT

The Channel Islands (San Miguel, Santa Rosa, Santa Cruz, and Anacapa) form an east-west ridge that, at intermediate levels, divides the Santa Barbara Channel from the remainder of the California Bight (Figure 1). The western boundary of the bight is formed by a submerged ridge projecting equatorward from Santa Rosa Island and including San Nicolas Island and Cortes and Tanner banks. This latter ridge, referred to as the Santa Rosa–Cortes (SR-C) Ridge [*Sverdrup and Fleming*, 1941] is perforated by gaps of various depths. To some degree these bathymetric features act as an impediment to the poleward-flowing CU.

It is desirable to use the greatest reference pressure available for the representation of dynamic height on the assumption that the relief in the pressure field at the deepest level is insignificant (i.e., that the absolute geostrophic velocities at this level are negligible for all practical purposes). It has long been held that a choice of 500 to 1000 dbar (1 dbar = 10^4 Pa) is sufficient for estimating the flow of shallow currents in the eastern North Pacific. A reference pressure of 1000 dbar (actually 1000 m, or approximately 1009 dbar) is available for stations west of the vicinity of the SR-C Ridge. Within the bight, however, the bottom depth is considerably less than 1000 m. There, 500 dbar has been chosen as a reference pressure. We present one set of maps of dynamic height using 500 dbar as a reference pressure and a second set using 1000 dbar, each to be applied in the appropriate region. Where a comparison can be made, the differences between the two are examined.

In three instances where an intermediate station in a line failed to reach 1000 m, we have used interpolation to fill in the missing values. We have also applied the method of extrapolating the

slope of deep isopleths of dynamic height [*Montgomery*, 1941; *Reid and Mantyla*, 1976] where the depth at the station at the end of a station line does not reach 1000 m. These extrapolations are confined to stations that fall upon the slopes of the SR-C Ridge. There are not enough stations that reach 1000 m within the bight to apply the method of extrapolation to those stations that fall along the coast. The results of this extrapolation of dynamic height are entirely consistent with the larger patterns.

5. RESULTS

5.1. *Patterns of Surface Circulation*

The pattern of flow, as given by the dynamic height of the sea surface relative to 500 dbar (Figure 2*a*), shows that the core of the CC lies 90 to 170 km off Point Conception. Between 31°N and 32°N the flow turns shoreward. The cyclonic flow about the outer banks is the Southern California Eddy (SCE). Its center encircles San Nicolas Island. The flow in the coastal zone is weakly equatorward. The major features of the distribution of salinity at the shallow salinity minimum reflect the pattern of surface flow (Figure 2*b*). In general, the minimum in salinity is found at the sea surface north of Point Conception. South of Point Conception, saline surface waters of both the central eastern North Pacific and the upwelled coastal waters mix with and override the low-salinity core of the CC to form a shallow subsurface minimum in the upper thermocline [*Reid et al.*, 1958, 1964]. Except for a single station in the northwest corner of our station grid, the salinity minimum in the CC is subsurface (20 to 75 m) (Figure 2*b*). The shoreward sweep of the CC and the inshore limb of the SCE bring the shallow subsurface salinity minimum into the California Bight. Upwelling in the center of the cyclonic SCE brings the minimum to the sea surface north and east of San Nicolas Island (indicated by asterisks in Figure 2*b*). Thus upwelling within the SCE was stronger than along the coastal margin during the observational period.

Beam transmission provides an independent tracer of flow. Figure 2*c* shows the depth integral of the beam attenuation coefficient for the upper 100 m. There is a very narrow tongue of relatively turbid water having values of integrated beam coefficient in excess of 12 lying immediately seaward of the SR-C Ridge (Figure 2*c*). In contrast to these turbid waters, the CC carries a broad tongue of relatively clear oceanic waters (values less than 8) which sweeps shoreward and penetrates into the middle of the bight.

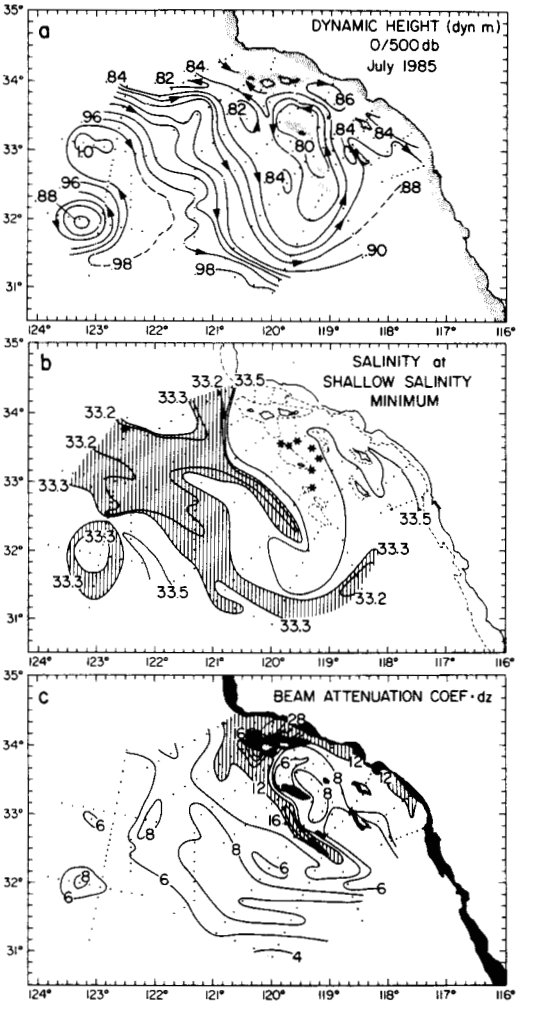

Fig. 2. (*a*) Dynamic height (dynamic meters, or 10 $m^2 s^{-2}$) of the sea surface relative to 500 dbar. The bathymetry in this and subsequent figures of dynamic height is shown stippled. (*b*) Distribution of salinity at the shallow salinity minimum. The depth of this feature was generally less than 70 m. At eight stations (shown by asterisks) the minimum occurred at the surface. (*c*) Beam attenuation coefficient (units of reciprocal meters) integrated over the upper 100 m of the water column. Bathymetry in this and subsequent figures of distributions is shaded black.

5.2. *Patterns of Subsurface Circulation*

The most energetic flow, indicated by closely-spaced contours of dynamic height at 250 m relative to 500 dbar (Figure3*a*), occurs where the poleward-flowing CU hugs the continental slope. The main flow of the CU appears to exit the bight through the gap in the bathymetry between Santa Rosa Island and San Nicolas Island. The data also imply that part of the CC at this level turns into the bight, swings poleward, and exits the bight through a gap south of San Nicolas Island where it then joins the CU. The distributions of salinity and dissolved oxygen on the surface where σ_t = 26.6 (Figures 3*b* and 3*c*) show that the waters having the highest salinities (shaded for values above 34.2) and the lowest oxygens (shaded for values below 1.4 mL L^{-1}) are found along the path of the CU. These waters also are found within the gap north of San Nicolas Island and extend northwest from there along the continental slope of the west end of the Channel Islands. Within most of the domain of the CU this σ_t surface lies between 260 and 300 m. Waters of nearly the same characteristics are found in the Santa Barbara Channel (Figure 3). The sill depth of the eastern end (230 m) precludes significant flow at this density. Some small flow, however, may occur up and over the sill.

5.3. *Controlling Bathymetry*

Silhouettes of the controlling bathymetry (Figure 4) show that the sill depths in the gaps in the SR-C Ridge range between 362 and 480 m (excluding the shallow dip between the Cortes and

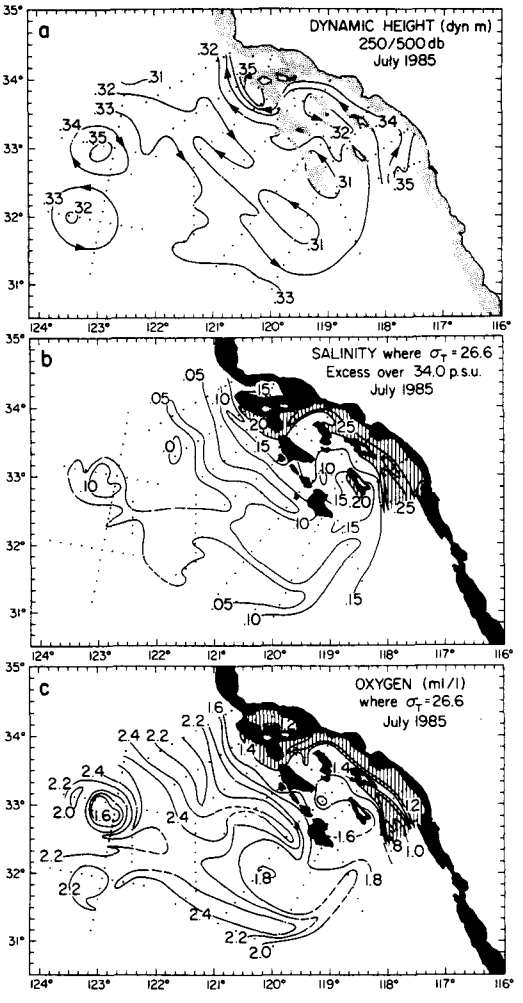

Fig. 3. (*a*) Dynamic height (dynamic meters, or 10 m^2 s^{-2}) at 250 m relative to 500 dbar. (*b*) Salinity (as excess over 34.00 psu on the surface where σ_t = 26.6. Salinities greater than 34.2 are shaded. (*c*) Oxygen concentration (mL L^{-1}) on the surface where σ_t = 26.6. Oxygen less than 1.4 mL L^{-1} is shaded.

Tanner banks). The sill depth in the gap between the islands of Santa Rosa and San Nicolas is 436 m. The opening at the western end of Santa Barbara Channel is deep (474 m) and broad, while at the eastern end it is relatively shallow (230 m) and more restricted.

5.4. *Velocity Sections*

The vertical sections of relative geostrophic velocity (Figure 5; locations shown in Figure 1) in the regions west of the SR-C Ridge exhibit bands of poleward and equatorward flow. The vertical maxima in equatorward flow (0.16 to 0.24 m s^{-1}) occur at the surface. Except for flow associated with the SCE, poleward maxima (0.06 to 0.18 m s^{-1}) occur at depths of 65 to 550 m. Within the bight the relative geostrophic velocity is almost totally poleward (Figure 5, section II). There are two maxima; the one at the surface (0.18–0.24 m s^{-1}) is the eastern limb of the SCE, and the other at 65 m (0.28 m s^{-1}) lies above the continental slope within the San Pedro Channel (between Santa Catalina Island and the mainland). The two pairs of stations that adjoin both sides of Santa Catalina have a deep poleward velocity maximum, between 200 and 240 m. The deep penetration of vertical shear evident in the San Pedro Channel suggests that there may be appreciable slope to the pressure field at 500 dbar. Hence the velocity of the CU may be underestimated there.

5.5. *Dynamic Height Relative to 1000 dbar*

The dynamic height of the sea surface relative to 1000 dbar [see *Simpson and Lynn*, this issue, Figure 9*a*] has some differences from the version using a 500-dbar reference (Figure 2*a*). Greater differences, however, are more evident at the 250-m level (Figures 3*a* and 6). Overall, there is greater topographic relief when using the greater reference pressure. The enhanced gradients in dynamic height (relative to 1000 dbar) off San Diego and south of Santa Cruz Island reveal that the CU is stronger than that indicated by using the 500-dbar reference pressure. At 250 m over 1000 dbar the CC is not a continuous flow. At this depth, most of the equatorward flowing waters appear to turn about and join the poleward flow. The SCE is not found at this level. In its place there is westward flow through gaps in the SR-C Ridge. There is a strong cyclonic eddy (marked with an E in Figure 6) centered at 31°35'N, 119°40'W which differs markedly from the surface pattern. This deep eddy has an elongated east-west configuration.

5.6. *Water Mass Characteristics*

Vertical sections of characteristics are dominated by the usual strong vertical gradients. An effective method to examine isopycnal distributions of water mass characteristics is to remove these strong diapycnal trends. This is done by calculating the anomalous differences between characteristic curves (T versus S, O_2 versus σ_t) for station data and specified mean characteristic curves. The resulting anomalies can be plotted as vertical sections and maps to reveal the distributions of the different water masses. We have chosen to create mean characteristic curves for the core region of the CC as a basis for calculating the anomalies. This choice causes the largest anomalies in this data set to occur in the CU. Figure 7 shows the location of 39 stations that were selected as most representative of the local CC for creating the mean curves. The stations selected fell within the broad southeastward flow of the CC as seen in the pattern of dynamic height (Figure 2*a*). This selection excludes stations in the SCE and eddy E because they entrain coastal waters. Also excluded were stations in the northwest and within and about the eddy dipole because of strong interleaving and entrainment of differing water types. The cast data and calculated parameters for the 39 stations were interpolated and averaged at intervals of 0.01 in σ_t. The resulting curves (heavy lines in Figures 8*a* and 8*b*) are smooth with very shallow inflections. The envelope of the variation of the 39 stations (depicted by shading) is narrow, indicating that we have identified a local water mass. The characteristic curves for station 19, located in the San Pedro Channel (Figure 7), are also shown in Figures 8*a* and 8*b* (light lines) for comparison. This station is representative of near-coastal waters. Waters at station 19 are warmer and more saline than the 39-station average for any given density. Lines of constant σ_t (labeled 23 through 27) are

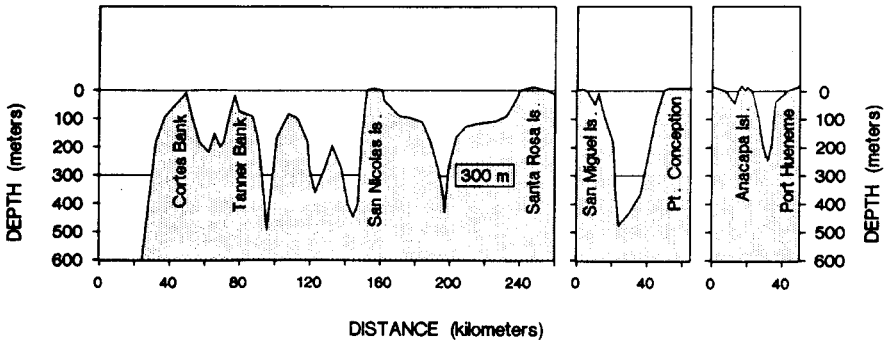

Fig. 4. Silhouettes of bathymetry showing the controlling sill depths along the Santa Rosa–Cortes (SR-C) Ridge and both ends of the Santa Barbara Channel.

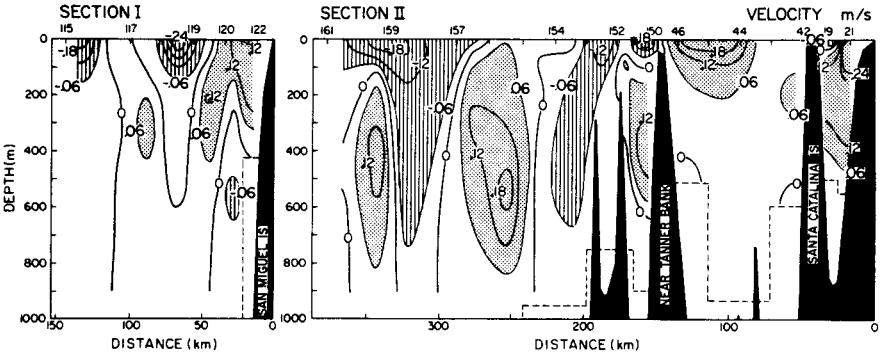

Fig. 5. Vertical sections of relative geostrophic velocity (in m s^{-1}). Locations of sections are given in Figure 1 (Roman numerals). Velocities greater than 0.06 m s^{-1} are hatched (equatorward) and stippled (poleward).

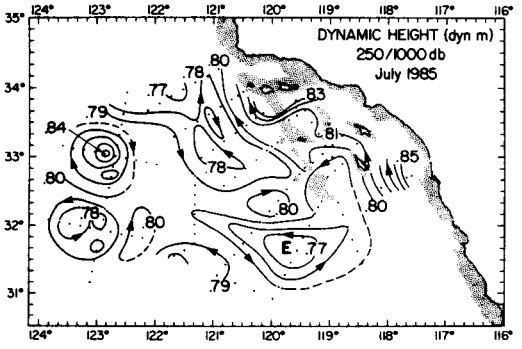

Fig. 6. Dynamic height (dynamic meters, or 10 m^2 s^{-2}) at 250 m relative to 1000 dbar. E denotes the center of a subsurface eddy.

given in Figure 8*a*. The set of lines that are nearly orthogonal to σ_t represents constant values of spiciness (labeled -1 through 3). Spiciness (symbol π), a function of temperature and salinity, was formulated to scale temperature–salinity differences along lines of constant σ_t [*Stommel*, 1962; *Munk*, 1981]. We calculate spiciness by the method of P. Flament (A note on seawater spiciness and diffusive stability, submitted to *Deep-Sea Research*, 1989). A concise mathematical definition of spiciness based upon Flament's derivation is given by *Simpson and Lynn* [this issue]. We use it as a tracer to measure the deviation of water characteristics from a mean *T–S* curve. In this context, waters having a positive anomaly of spiciness are both warmer and more saline than the chosen standard; and vice versa. The deviation or anomaly of station 19 from the mean *T–S* curve at a level where $\sigma_t = 26.6$ is shown in Figure 8*a*. This anomaly shows the difference between CC and CU waters ($\sigma_t = 26.6$ occurs at 260 m for station 19). At densities less than $\sigma_t = 25.6$, station 19 has higher values of dissolved oxygen than the 39-station mean; at greater densities it is the reverse (Figure 8*b*). CU waters at $\sigma_t = 26.6$ have an oxygen anomaly of approximately -1 mL L^{-1}.

Although station 19 is more spicy than the 39-station mean at any given density (Figure 8*a*), it has layers that are both more and less spicy as a function of depth (Figure 8*c*). This difference is a consequence of the overall upward tilt toward shore of the density field in response to large-scale dynamics. If anomalies are computed using depth as the ordinate, the result combines the effects of both the geostrophic (vertical) displacement of the density field and the water mass differences seen in *T–S* diagrams.

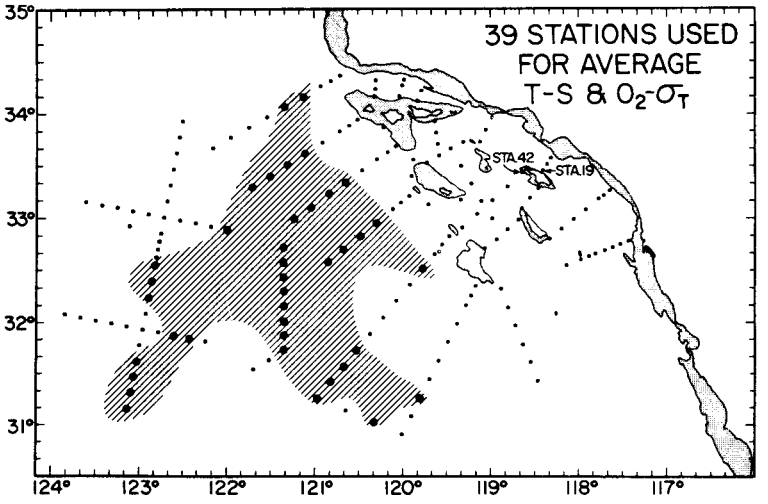

Fig. 7. Location of 39 stations used to create mean T–S and O_2–σ_t curves.

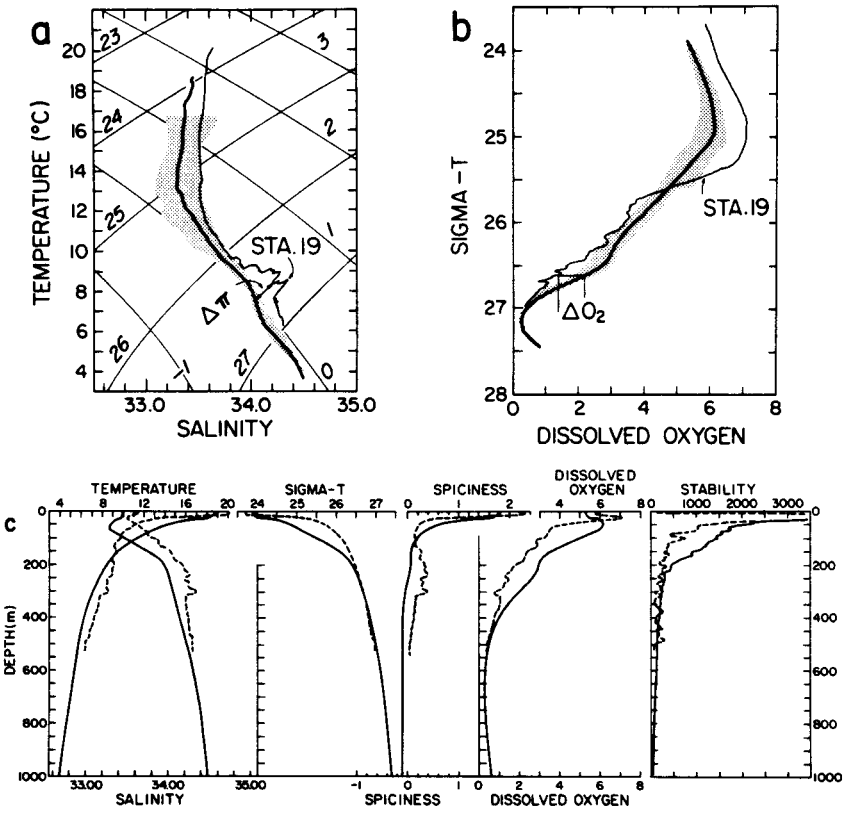

Fig. 8. (*a*) Temperature–salinity diagram with lines of σ_t (labeled 23 to 27) and spiciness (labeled -1 to 3). The average curve for the 39 stations of Figure 7 is given by the heavy line, and the range is shown by shading. Station 19 is given by the thin line. The difference in spiciness ($\Delta\pi$) between these curves at σ_t = 26.6 is shown. (*b*) The same as Figure 8*a*, except for σ_t versus oxygen. (*c*) Vertical profiles of characteristics for the 39-station averages (solid lines) and for station 19 (dashed lines). All averaging (including depth) was done at common levels of σ_t. Hydrostatic stability has units of $m^{-1} \times 10^8$.

5.7. *Vertical Sections of Anomalies*

The largest anomalies of spiciness (>3) and dissolved oxygen (<-9) occur in the southern part of the bight in layers at intermediate depths (section III, Figure 9; location of sections given in Figure 1). These and all other anomalies reported herein are multiplied by 10. Without further specification, dissolved oxygen anomaly is given as $\times 10$ mL L^{-1}, and spiciness anomaly is given in $\times 10$ units of σ_t. Peak values of positive spiciness anomaly occur near 350 m, and those of negative oxygen anomaly occur near 230 m. These subsurface layers of extremes are also found outside of the SR-C Ridge, off San Miguel Island (section I, Figure 9) where their extreme values (at reduced levels) are confined within 60 km of the continental slope. Section II of Figure 9 offers a broader perspective of the distribution of anomalies. It transects the entire bight near midpoint and also most of the CC and is approximately coincident with CalCOFI line 90. Layers of subsurface anomaly extrema (positive spiciness and negative dissolved oxygen) occur throughout the bight and beyond, with the most extreme values found over the continental slope (in the San Pedro Channel). In this figure anomalous values (1 in spiciness and -3 in oxygen) extend over 280 km from shore (to station 157). In the surface domain (<75 m) the spiciness is particularly high, commensurate with the higher values of temperature and salinity caused by surface warming and evaporation and/or mixing. The shallow waters also have greater dissolved oxygen because of local biological and physical processes. Between the shallow and deep maxima in spiciness in the bight there is a minimum layer

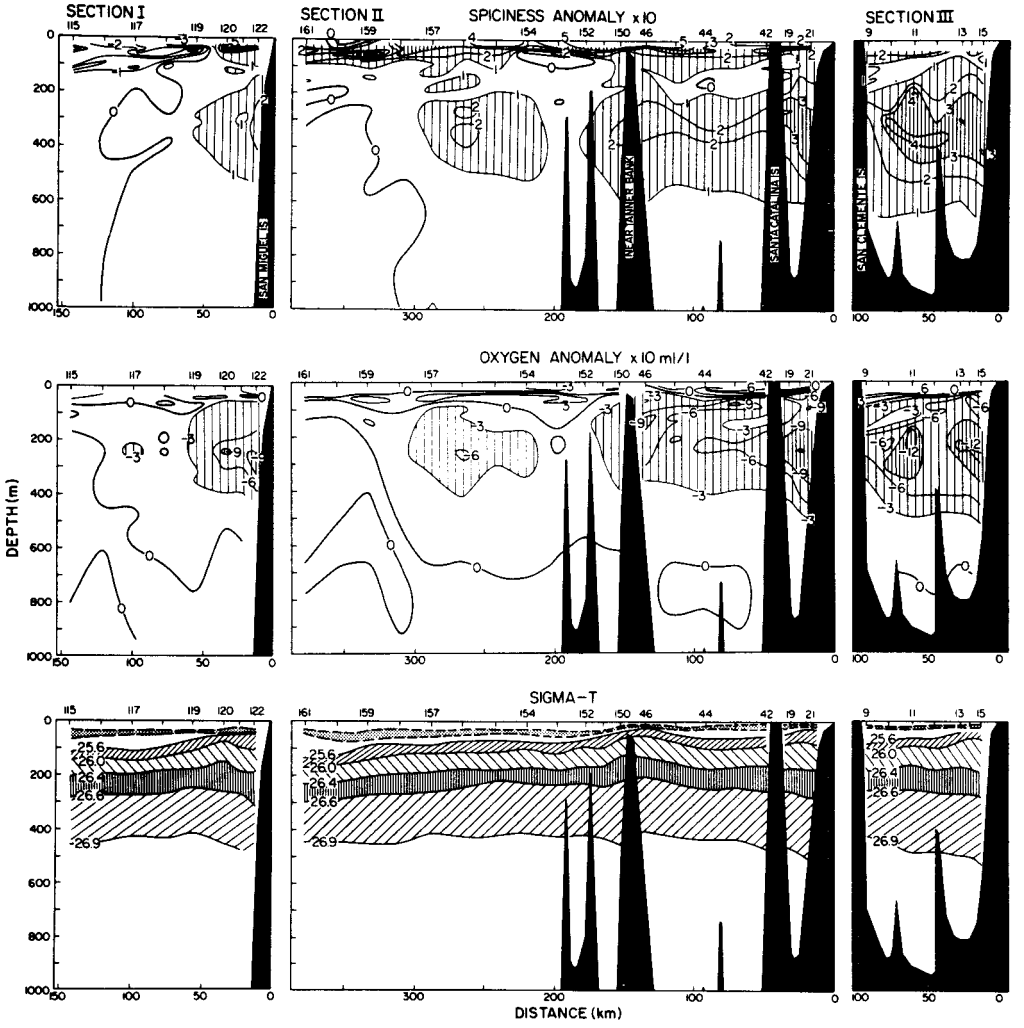

Fig. 9. Vertical sections (lines I, II and III of Figure 1) of spiciness anomaly $\times 10$ units of σ_t, oxygen anomaly $\times 10$ mL L^{-1}, and σ_t. Anomalies of spiciness above 1.0 and of oxygen below -3.0 are hatched. The shallow shaded layer in σ_t is the strong summer pycnocline. The four layers in σ_t that are identified in the text are indicated by differing manners of hatching.

which is more indicative of offshore waters. The oxygen anomaly pattern associated with the spiciness minimum layer differs from that of spiciness; the complex biological processes active there override the influence of transport and lateral mixing.

5.8. *Maps of Anomalies*

Four density layers, σ_t = 25.6 to 26.0, 26.0 to 26.4, 26.4 to 26.6, and 26.6 to 26.9, were selected for mapping the distribution of anomalies. Average anomaly values within these layers, rather than values at a specified σ_t surface, were used to avoid variations associated with small-scale processes that cannot be resolved by the given station spacing. These layers are centered about depths of 80, 140, 200, and 350 m, respectively (Figure 9c) and hereinafter are referred to as layers 1 through 4. Layer 1 lies close enough to the surface that its characteristics are affected by diapycnal mixing as well as by lateral mixing and transport, whereas in the deeper layers lateral mixing and transport are the dominant processes. The anomalies of spiciness and dissolved oxygen for layers 1 through 3 are given in Figures 10 through 12. Layer 4 is discussed but not shown. A map of acceleration potential [*Montgomery*, 1937; *Montgomery and Stroup*, 1962] for the σ_t surface found at depths that are intermediate within layer 1 is also presented (Figure 10*a*). Maps of acceleration potential (in units of dynamic meters, or 10 m^2 s^{-2}) provide the patterns of geostrophic flow for surfaces of variable depth.

5.8.1. *Layer 1 (σ_t = 25.6 to 26.0).* The pattern of geostrophic flow on the surface where σ_t = 25.8 relative to 1000 dbar (Figure 10*a*) differs appreciably from that found at the sea surface relative to 500 dbar (Figure 2*a*). This density surface (midway in the depth range of layer 1) is found near 50-m depth both inshore and in the SCE, and near 100- to 150-m depth offshore. From the sea surface to this density surface there is an overall decrease in geostrophic flow within the CC proper. The center of the SCE has shifted southward from San Nicolas Island to the Tanner and Cortes banks. Eddy E appears as a separate cyclonic eddy southwest of the SR-C Ridge.

Within layer 1, relatively spicy (warm and saline) waters are found along the coast and within eddy E (Figure 10*b*). The most extreme values of positive spiciness, >2, occur within the SCE and about the SR-C Ridge. The pattern within eddy E shows relatively spicy waters projecting westward from the southern end of the SR-C Ridge. Waters of relatively low spiciness penetrate from the northwest in the core of the CC. The CC waters also have relatively high dissolved oxygen in layer 1 while the waters in the bight exhibit low oxygen. The distribution of oxygen anomaly, however, shows only a very weak correspondence to that of the spiciness anomaly.

5.8.2. *Layer 2 (σ_t = 26.0 to 26.4).* The middepth of layer 2 (Figure 11) lies between 100 and 175 m. In layer 2 the spiciest and least oxygenated waters occur along the coast, penetrating northward from south of the international border. At slightly lesser values of the anomalies, spicy, low-oxygen waters lie along and on both sides of the SR-C Ridge and project westward from the southern extent of the ridge. The zero contour of spiciness anomaly forms a mushroom-shaped pattern which extends into the eddy dipole system [*Simpson and Lynn*, this issue]. The oxygen anomaly shows a similar symmetrical pattern. Waters having low values of anomalies penetrate the central bight from the southwest. The distributions of spiciness and oxygen are very similar.

5.8.3. *Layer 3 (σ_t = 26.4 to 26.6).* The middepth of layer 3 (Figure 12) lies between 200 and 260 m. Overall, the distributions of anomalies are similar to those of the layer 2, above. The range of anomalies in layer 3, however, is much greater. The maximum spiciness is 4, where it had been 2 in layer 2. The waters that exceed 2 are continuous along the coast, through the gap south of Santa Rosa Island and northward along the SR-C Ridge. The dissolved oxygen deficit reaches its maximum value at this level, -14. The symmetry in the dipole eddy anomalies observed in layer 2 is absent in layer 3.

5.8.4. *Layer 4 (σ_t = 26.6 to 26.9).* The middepth of layer 4 (not shown) lies between 300 and 400 m. The pattern of the spiciness anomaly is very similar to that for layer 3, differing only in that the anomalies are slightly greater in the gap south of Santa

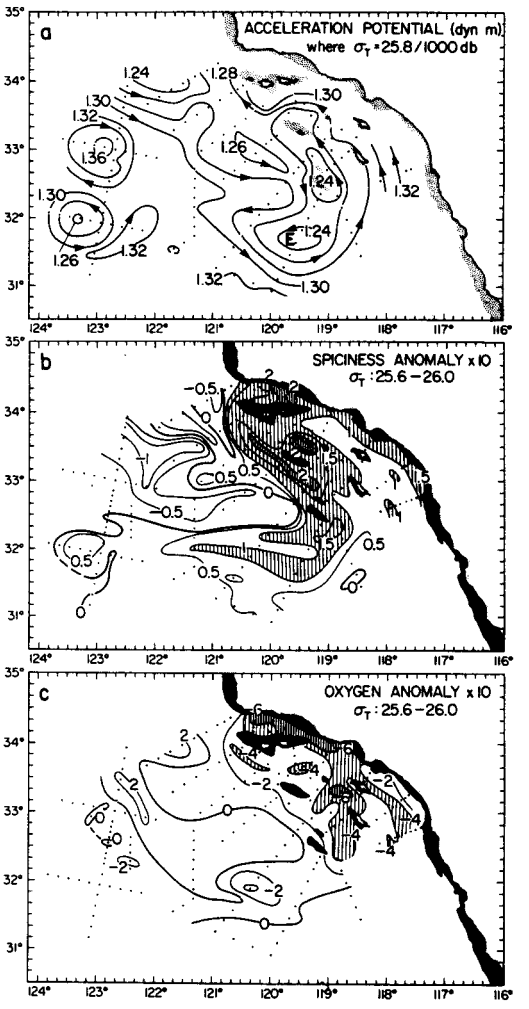

Fig. 10. (*a*) Acceleration potential (dynamic meters, or 10 m^2 s^{-2}) at the surface where σ_t = 25.8 relative to 1000 dbar. E denotes the center of a subsurface eddy. (*b*) Anomaly (from the 39-station mean) of spiciness × 10 units of σ_t averaged over a range in σ_t of 25.6 to 26.0 (layer 1). Positive anomalies in excess of 1 are hatched. (*c*) Anomaly of oxygen concentration × 10 mL L^{-1} as above (layer 1). Negative anomalies below -4 are hatched.

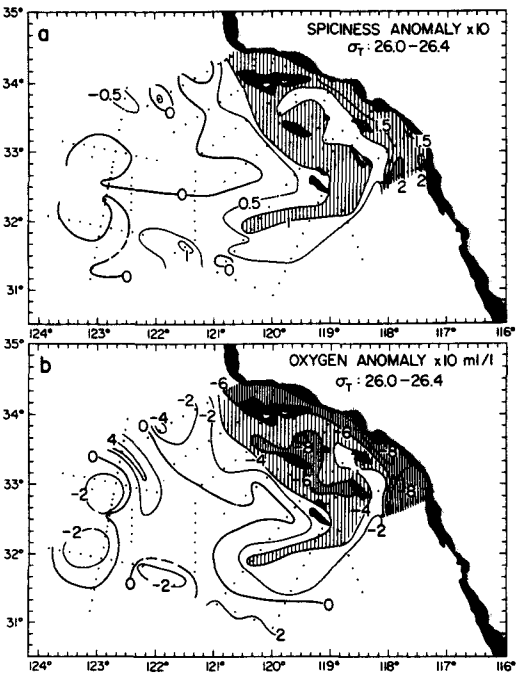

Fig. 11. (*a*) As per Figure 10*b*, except for a range in σ_t of 26.0 to 26.4 (layer 2). (*b*) As per Figure 10*c*, except for a range in σ_t of 26.0 to 26.4 (layer 2).

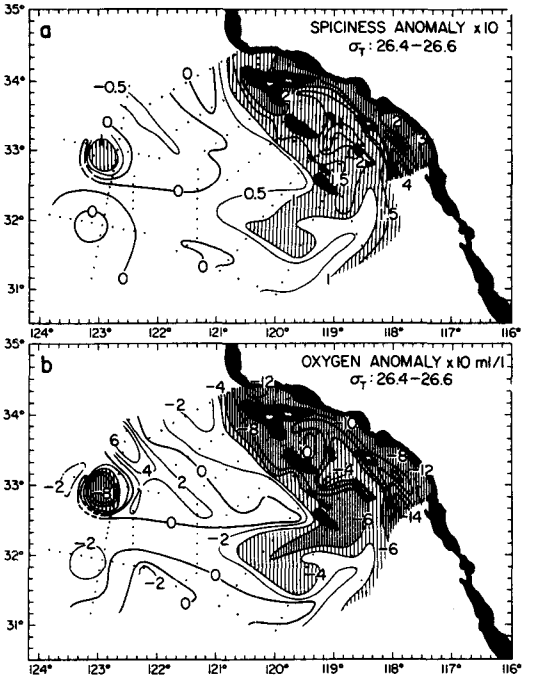

Fig. 12. (*a*) As per Figure 10*b*, except for a range in σ_t of 26.4 to 26.6 (layer 3). (*b*) As per Figure 10*c*, except for a range in σ_t of 26.4 to 26.6 (layer 3).

Rosa Island and in the offshore penetration in the northern limb of eddy E. While the overall pattern of the oxygen anomaly is similar to layer 3, the range is less than half.

6. DISCUSSION

6.1. *Path and Continuity of the California Undercurrent off Southern California*

The dynamic height at 250 m (Figures 3*a* and 6) reveals that the California Undercurrent is the strongest continuous flow at that depth. It follows the continental slope through the California Bight and exits the bight through the northernmost gap in the SR-C Ridge, and then continues poleward along the continental slope. The distributions of salinity and dissolved oxygen on the surface where $\sigma_t = 26.6$ (Figures 3*b* and 3*c*) confirm this path and the continuity of the CU. The characteristic extremes of relatively high salinity (hence relatively high temperature) and low oxygen and the decrease in their values along the path indicated by the dynamic height identify the waters as being of southern origin. The dynamic height patterns at 250 m suggest that there is poleward flow throughout much of the remainder of the bight, although at lesser speeds, and that there is westward flow out of each of the gaps. Mixing with waters that enter the bight from offshore sources reduces the extreme values of water characteristics in the more southerly gaps.

The density surface of 26.6 lies below the sill depth of the eastern entrance of the Santa Barbara Channel. Hence this surface does not show flow of the CU within the Santa Barbara Channel. At lesser densities the channel is open to flow (Figures 10, 11, and 12). Other data [*Kolpack and Drake*, 1985] provide additional evidence for a poleward, subsurface flow through the Santa Barbara Channel. We presume that the volume flow of the CU through the SR-C Ridge is considerably greater than that through the Santa Barbara Channel because of the greater restriction to flow imposed by the eastern entrance to the channel.

6.2. *Contrast of California Undercurrent Flow With Near-Surface Flow*

The CU is identified in section II of Figure 5 by the subsurface maxima in poleward geostrophic velocity found at intermediate depths within the San Pedro Channel (>0.12 to >0.24 m s^{-1}), immediately to the west of Santa Catalina Island (>0.06 m s^{-1}) and to the northwest of Tanner Bank (>0.12 m s^{-1}). The poleward flow is, in fact, continuous across the bight at these depths. In the southern part of its path through the bight, the strong core of the CU underlies a weak, spatially incoherent coastal surface flow (Figure 2*a*). In the northern part of the bight and in the northernmost gap in the SR-C Ridge the CU underlies strong surface flow that is coincident in direction and associated with the northern limb of the SCE. Westward, beyond the gap, the CU turns poleward (Figure 6) while the surface flow divides (Figure 2*a*); the major portion of this surface flow is retained in the SCE.

Although there is a general correspondence of poleward flow in the bight between the sea surface and 250 m, there is considerable difference with depth in the detail of the patterns of flow. In a matter of some tens of meters below the surface, circulation pat-

terns change (Figures 2*a* and 10*a*). Near 50-m depth a greater portion of the flow exiting the northern gap turns poleward, and the center of the SCE shifts southward from San Nicolas Island to Cortes Bank. Eddy E enlarges and intensifies with increasing depth, while the SCE weakens (Figures 10*a* and 6). At 250 m there is only a vestige of the SCE flow about Cortes Bank.

The CU is both a narrow energetic subsurface poleward flow concentrated over the continental slope and a broad weak poleward transport found out to 200 km from the coast. The offshore CC is regarded as a relatively shallow flow [*Reid et al.*, 1958]. The present data show that at 250 m the continuity of the CC is replaced by largely eddylike flow (Figure 6). At this depth the dynamic height indicates that much of the waters from the north and northwest turn about and join the CU at various latitudes.

6.3. *Correspondence of Velocity and Anomaly Patterns*

There is a general correspondence between the high values of subsurface poleward flow (section II, Figure 5) and high values of positive spiciness anomaly and negative oxygen anomaly (section II, Figure 9). The anomalies are greatest nearest the continental slope and, at slightly lesser values, are found in a layer at intermediate depths across the bight and immediately westward of the SR-C Ridge. Both the velocity structure and the anomaly patterns indicate the presence of a branch of the CU to the northwest of Tanner Bank. This finding is supported by the pattern of dynamic height at 250 m (Figure 6) where a contour labeled 0.8 dyn m passes San Clemente Island, exits the bight through a gap north of Tanner Bank, and continues poleward. A similar correspondence of flow and anomaly patterns is evident west of San Miguel Island (section I, Figures 5 and 9).

An exception to the correspondence of patterns of extrema in velocity and anomalies occurs over the continental slope in section II, Figure 5. The velocity maximum there (0.24 to 0.28 m s^{-1}), at 65-m depth, is well above the depths of the extrema in anomalies and appears to be recirculation of mixed waters within the bight.

Of the two additional bodies of strong subsurface poleward flow in section II, Figure 5, the one at a distance of 250 km from the coast is associated with anomalously spicy and low-oxygen water, and the other at 340 km is not (Figure 9). The one located at 250 km is a part of eddy E (Figure 6). At 250-m depth the geostrophic velocity perpendicular to this section is 0.11 to 0.12 m s^{-1} in both limbs of eddy E. The subsurface velocity maximum located at 340-km distance appears to be an eddy or meander carrying typical CC waters. This feature is too close to the edge of the station grid to be resolved by these data.

6.4. *The Lateral Spread of CU Waters*

The four density layers chosen for the analysis of water characteristics can be seen to encompass the range of depth of the layers of anomaly extremes (Figure 9). In the following discussion they are taken in sequence starting with the surface domain and layer 1.

Eddy-induced upwelling and divergence within the cyclonic SCE disperses surface waters so as to eliminate the subsurface salinity minimum (Figure 2*b*) and bring relatively high salinity waters to the surface. The doming of the salinity structure within the SCE and near-surface turbulent mixing enhances the downward transport of heat from the surface and produces an isolated maximum in spiciness anomaly in layer 1 (Figure10*b*). Wind-induced upwelling combined with surface heat exchange and vertical mixing may also account for the greater spiciness of this layer in the Santa Barbara Channel and in the coastal strip. The northward penetration within the center of the bight of water with spiciness anomalies of <1 separates the effects of coastal events from those of the SCE. The tongue of values greater than 0.5 that projects offshore from the southern end of the SR-C Ridge must have formed as a result of offshore transport. Eddy E is relatively well defined at this level (approximately 70 m). Further, the western part of the tongue lies between 100 and 140 m and underlies the southeast transport of the low-salinity core of the CC. In layer 1 the spatial patterns of the anomalies of spiciness and dissolved oxygen do not match, especially within the bight. This condition suggests that local near-surface processes, including biological processes, and vertical exchange have a significant effect upon the distributions and lateral transport has a minor role.

Layer 2 encompasses a vertical minimum in spiciness anomaly over most of the survey area (Figure 9). The minimum is maintained by southward and onshore transport of CC waters which are relatively isolated from the most immediate effects of near-surface processes. Only within the coastal strip does the minimum lie above layer 2. The relatively large spiciness anomaly, >2, and large oxygen anomaly, <-8, entering the grid from south of San Diego at approximately 122 m is the upper part of the CU water mass. The similarity of the patterns of the anomalies, their close match to the pattern of acceleration potential (shown only for layer 1), and the downstream gradation of these values from off San Diego along the general path of flow, all point toward lateral transport as the primary determinant of these patterns.

The magnitude of the anomalies in layer 3 (Figure 12) is about twice that of layer 2. The oxygen anomaly, in particular, has its largest range of extremes in layer 3, from 6 in the CC waters entering from the northwest to -14 in the CU waters entering from the southeast. This large range provides the strongest development of the characteristic pattern of anomaly distribution, and this is the best of the four layers for tracing the flow of the CU. A core of large values of positive spiciness anomaly and negative oxygen anomaly, which gradually diminish along its path, follows the continental slope northward, across the bight south of the Channel Islands and out through the northern gap in the SR-C Ridge where it turns northward again. Moderately large values of anomalies also continue southward along the SR-C Ridge, then offshore in a tongue projecting westward from the southern end of the ridge. CC waters from the north, identified by anomalies of opposite sign to those of the CU, enter the grid from the northwest. Waters of intermediate anomaly values penetrate the center of the bight as they do in shallower layers, but they have assumed more of the characteristics of CU water in this layer. Large values of anomalies, indicative of CU waters, also continue into the Santa Barbara Channel (which is open on its eastern end for most (but not all) of the depth range of layer 3.

Layer 4 encompasses the deeper portion of CU water as identified by water mass characteristics (Figure 9). The distribution patterns of anomalies are much the same as those in the overlying waters.

6.5. *Eddy E*

The SCE is a shallow eddy with its maximum velocities at the surface, whereas eddy E is deeply rooted with its maximum velocities at depths greater than 200 m. It does not appear, therefore, that these features have a direct association. Rather, eddy E appears to have developed from baroclinic instabilities that are centered in the depth range of the CU. The patterns of geostrophic circulation and anomalies provide strong evidence that

baroclinic instabilities develop in the CU at this locale as a result of the presence of the large bathymetric features in the SR-C Ridge. The configuration of eddy E and the offshore protrusion of waters of CU origin indicate a major offshore discharge of subsurface waters of near-coastal origin toward the region of the eddy dipole.

At a position 250 km offshore in section II of Figure 5 there is a maximum in geostrophic velocity (>0.18 m s^{-1}) at a depth of 550 m. The position of this finding, 32°08'N, 120°08'W, falls between the northern limb of eddy E and the southern limb of an adjacent small anticyclonic eddy. At a depth of 500 m, the dynamic height relative to 1000 dbar (Figure 13) shows, in fact, that eddy E is relatively weak and the anticyclonic eddy is strong.

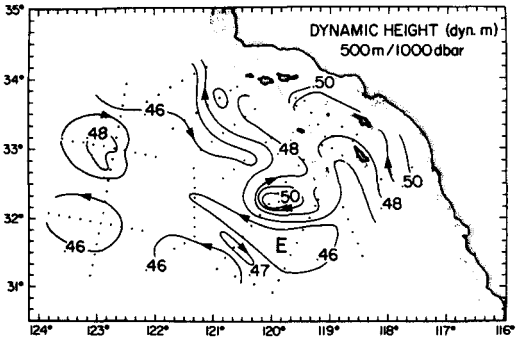

Fig. 13. Dynamic height (dynamic meters, or 10 m^2 s^{-2}) at 500 m relative to 1000 dbar.

The line of stations that comprises section II (Figure 1) misses the center of eddy E (Figure 6). The geostrophic velocity section for the line of stations that does bisect eddy E (not shown) demonstrates that the maximum in rotational velocity of eddy E occurs between 200 and 250 m, a range of depth that includes the maxima in the anomalies of spiciness and oxygen. At 500 m and below, the SR-C Ridge appears as an unbroken submerged peninsula. Flow at 500 m (Figure 13) appears to enter the bight from the south along the continental margin. It must exit the bight around the southern end of the SR-C Ridge, in the vicinity of the deep anticyclonic eddy. The anticyclonic eddy, by virtue of its proximity to the SR-C Ridge and its spatial scale, may also have been created by a bathymetrically induced instability in flow.

6.6. *Offshore Transport of CU Waters*

The offshore transport of CU waters that these survey data reveal is likely episodic in nature. Therefore this single realization of flow and water mass distribution does not permit definitive conclusions as to its development and evolution. Our findings combined with background information do, however, provide some evidence as to the probable turn of events. In the vicinity of the international border the seasonally averaged CU attains its minimum strength (or disappears altogether) during April and undergoes its greatest increase during June and July [*Lynn and Simpson*, 1987]. We reason that the effect of the impediment of the SR-C Ridge on the CU is greatest during this period of seasonal intensification of baroclinic flow. The possible accumulation of CU waters at depth within the bight because of the constriction of the gaps in the ridge would ultimately lead to the discharge of these waters around the southern end of the ridge. Interaction of the offshore discharge of CU waters with the offshore flow field could produce a feature like eddy E as well as the deeper anticyclonic eddy noted in Figure 13.

CU-derived waters form the core of the anticyclonic member of the eddy dipole [*Simpson and Lynn*, this issue]. This concentration of anomalous waters within the anticyclonic member of the eddy dipole suggests that this system was generated near the continental slope. The patterns of subsurface anomalies indicate a path between the southern end of the SR-C Ridge and the eddy dipole (Figures 11 and 12). *Simpson et al.* [1984] also found waters of CU origin within a monopole eddy in nearly the same location as the anticyclonic member of the dipole. These findings imply that undercurrent dynamics play a crucial role in the development of offshore mesoscale eddies. The patterns found in July 1985 provide circumstantial evidence which suggests that the eddy dipole was generated off the SR-C Ridge and migrated westward to its offshore position, leaving in its wake mixed waters which included some CU waters. A recurrent mesoscale eddy found off Sitka, Alaska, also contains waters within a similar depth–density realm that have characteristics indicating an origin of the shelf–slope region [*Tabata*, 1982] and similar observations were made of an eddy off Oregon in early 1978 [*Huyer et al.*, 1984]. A mathematical model of the Sitka eddy [*Swaters and Mysak*, 1985] suggests that it is bathymetrically induced.

6.7. *Depth Offset of Extremes in Anomalies of Spiciness and Oxygen*

The relationship between the spiciness anomaly and oxygen anomaly is represented in Figure 14 by vertical traces for station 42, located immediately west of Santa Catalina Island (see Figure 7). The previously defined four density layers are indicated by five ticks on the zero axis. Below 60 m and at densities greater than 25.8 there is a strong negative correlation between the anomalies as expected for CU waters. Above 60 m the correlation is positive. This break point occurs at about the bottom of the thermocline–pycnocline and indicates the depth of penetration of

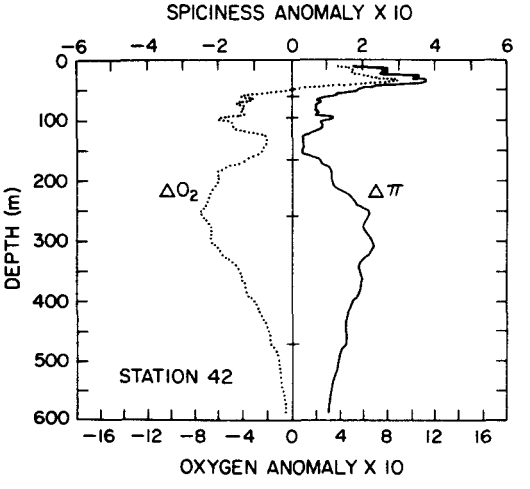

Fig. 14. Vertical profiles of the anomalies of spiciness ($\Delta\pi$) and dissolved oxygen (ΔO_2) from the 39-station mean for station 42 (west of Santa Catalina Island).

local exchange processes and strong vertical mixing. At some other stations, especially those in the SCE, the break point falls well into layer 1. At depths below this break point, large-scale transport and lateral mixing predominate. The negative correlation of anomalies is seen both in general form and in detail on a scale of 10 m. There is, however, a decreasing trend with increasing depth in the ratio of oxygen anomaly to spiciness anomaly. This trend causes the maximum oxygen anomaly to occur at a shallower depth than that for the spiciness anomaly. This trend most likely is simply a consequence of basic differences in the vertical distributions of spiciness and dissolved oxygen of the CC and CU source waters.

6.8. *Comparison of July 1985 With Long-Term Mean*

In order to compare our results for July 1985 with the long-term mean (LTM), we used the 29-year mean July values of temperature, salinity, and dissolved oxygen for CalCOFI line 90 [*Lynn et al.*, 1982] to compute spiciness and the anomalies of spiciness and dissolved oxygen from the 39-station spatial mean. The vertical sections of these anomalies (Figure 15) have a vertical exaggeration 8 times greater than for those presented earlier (Figures 5 and 9). Section II of Figure 9 nearly aligns with CalCOFI line 90 and extends westward to station 80. The full westward extent of the July 1985 grid reaches 570 km offshore, a position between CalCOFI stations 100 and 110, and the locale of the 39 stations used to create the mean CC characteristics falls in the region of CalCOFI stations 60 to 90. The patterns of the LTM anomalies (Figure 15) are very similar to those found in 1985 (Figure 9). In particular, in the LTM as in 1985, waters having anomalies >1 in spiciness and <-3 in oxygen extend 300 km offshore within layers 3 and 4; maximum values (>3 in spiciness and <-9 in oxygen) appear in the San Pedro Channel at about depths of 250 to 300 m. Spiciness is high in the surface waters, especially near the SR-C Ridge (CalCOFI station 53), where high values penetrate downward into layer 1. Also, there is an intermediate layer where spiciness is a minimum. Thus conditions observed in 1985 can be accepted as typical of the mean, especially the offshore extension of waters that carry a strong complement of CU characteristics.

Between 300 and 500 m at CalCOFI station 100, there is a separate body of water having anomalies >1 in spiciness and <-3 in oxygen (Figures 15*a* and 15*b*). This station is very near the location of the dipole eddy system. The vertical section of LTM July geostrophic velocity [*Lynn et al.*, 1982, plate on page 153] corresponding to the LTMs of temperature and salinity demonstrates a pattern of flow including a weak reversal that associates it with the separate body of anomalous water. Taken together, these findings strongly suggest that this separate feature is a subsurface signature of recurrent mesoscale eddies. Thus the findings attest to the recurrent nature of offshore mesoscale eddies at preferred locations [*Simpson et al.*, 1984, 1986; *Lynn and Simpson*, 1987] and strongly suggest that the offshore transport and eddy entrainment of CU-derived waters [*Simpson and Lynn*, this issue] is a common feature of the CCS.

6.9. *Comparison With North Pacific Eastern Central Waters*

To the west, the North Pacific Eastern Central waters have anomalies of spiciness and dissolved oxygen which clearly differentiate them from CC and CU waters (Figures 15*a* and 15*b*). The distinguishing features of CU waters are emphasized in

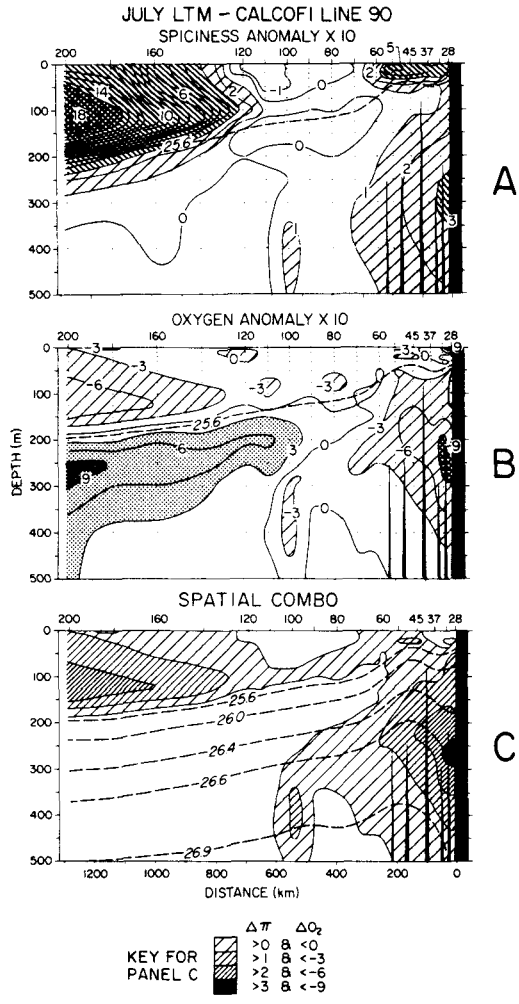

Fig. 15. (*a*) Vertical section of the anomaly of the long term mean (LTM) July spiciness for CalCOFI line 90 from the 39-station spatial mean. Various densities of hatching are used for values of 1–3, 3–15, and >15. (*b*) The same as Figure 15*a*, except for oxygen. Values >3 and <-3 are lightly shaded; values >9 and <-9 are heavily shaded. (*c*) The spatial combination of positive spiciness (π) anomaly and negative oxygen anomaly from Figures 15*a* and 15*b*. Contours are identified in key. Shading intensities grade accordingly.

Figure 15*c*, in which all waters that have a combined positive spiciness anomaly and a negative oxygen anomaly are shaded. The density of shading is stepped for combinations of anomaly values as given in the key. The maximum step, spiciness >3 and oxygen <-9, appears only over the continental slope between depths of 230 and 300 m. Within our chosen density layers there is no second source of waters having the same mean combination of characteristics as CU waters. (Seasonal and nonseasonal variations and dynamic events about the California Front, however, may occasionally produce such waters within layer 1.) Thus the

anomaly structures provide unambiguous evidence that both eddy E and the offshore eddy dipole contain CU waters. Necessarily, this implies a subsurface offshore transport mechanism.

7. CONCLUSIONS

1. The California Undercurrent transports spicy (warm and saline), low-oxygen waters poleward through the California Bight. The subsurface velocity core of this current is associated with vertical and lateral extremes in water characteristics that are readily defined by their anomalies from California Current waters. In July, at least, these extreme values of anomalies occur at or near σ_t = 26.6 and a depth of 275 m over the continental slope. The core, thus defined by flow and water characteristics, follows the continental slope within the bight, turns westward along the slopes south of the Channel Islands, exits the bight in the northernmost gap of the Santa Rosa–Cortes (SR-C) Ridge, and then turns northward. At levels above the sill depth of the eastern end of the Santa Barbara Channel (230 m) and at densities somewhat less than σ_t = 26.6, a branch of the CU continues northward along the continental slope into the Santa Barbara Channel.

2. At intermediate depths, typical of the CU, considerable portions of the CC waters turn cyclonically, mix with CU waters and join the CU. Thus there is both an energetic narrow core of poleward flow along the continental slope and a broad, somewhat slower, poleward flow that extends offshore to distances of the order of 100 to 150 km.

3. In July 1985 the flow within the bight was almost everywhere poleward. Branches of the CU in which its waters were diluted with offshore waters exited the bight through several gaps in the SR-C Ridge and merged again in a poleward flow. Part of the CU was diverted about the southern end of the ridge. There, eddying flow carried waters having a large component of CU water characteristics westward beneath the CC.

4. Waters of CU origin are transported offshore beneath the CC and are found in the offshore mesoscale eddy system [*Simpson and Lynn*, this issue]. This transport appears to result from baroclinic instabilities in the CU caused by the bathymetry and the seasonal intensification of flow. Distorted eddy-like features near the southern end of the SR-C Ridge are one manifestation of the baroclinic instabilities. The flow patterns of these features closely correspond to the distribution patterns of CU water characteristics, and together they indicate the path of offshore transport to the offshore mesoscale eddy field.

5. Circumstantial evidence suggests that the eddy dipole was generated off the SR-C Ridge and migrated westward.

6. The major aspects of the conditions found in July 1985 also appear in the long-term mean for July, including the magnitude and distribution of CU water characteristic anomalies, the association of these anomalies with the density field, and the entrainment of CU waters into the offshore mesoscale eddy system. Thus the findings for July 1985 appear to be typical conditions.

7. Long-term means of water characteristics in the eastern North Pacific show that the combination of relatively high spiciness and low dissolved oxygen uniquely define CU waters at densities greater than σ_t = 26 in the California Current system.

8. In some instances, a reference pressure of 500 dbar for the calculation of dynamic height off California does not provide an adequate representation of the strength and pattern of geostrophic flow. A very active pattern of geostrophic flow was observed at 500 m referred to 1000 dbar in July 1985.

Acknowledgments. The generous support by the late Reuben Lasker was instrumental in the initiation of this project. R.J.L. expresses his appreciation to R. M. Laurs for his unstinting support of this work. J.J.S. was sponsored in part by the Marine Life Research Group (MLRG) of the Scripps Institution of Oceanography, a grant from the California Space Institute, and an ONR-sponsored University Research Initiative (URI) to the Scripps Institution of Oceanography. The authors gratefully acknowledge the critical assistance of NOAA/NMFS/SWFC personnel, K. Bliss, L. Eber, P. Fiedler, and R. Nishimoto in the collection of the data, and the dedication and skill of Captain M. Roll, the officers and crew of the RV *David Starr Jordan* in the ship operations. S. McBride typed the manuscript. F. Crowe, G. Tapper, and N. Hulbirt assisted with figure preparation.

REFERENCES

Allen, W. E., Vernal distribution of marine plankton diatoms offshore in southern California in 1940, *Bull. Scripps Inst. Oceanogr., 5*, 335–369, 1945.

Chelton, D. B., Seasonal variability of alongshore geostrophic velocity off central California, *J. Geophys. Res., 89*, 3473–3486, 1984.

Davis, R. E., Drifter observations of coastal surface currents during CODE: The method and descriptive view, *J. Geophys. Res., 90*, 4741–4755, 1985.

Hickey, B. M., The California Current system—hypotheses and facts, *Prog. Oceanogr., 8*, 191–279, 1979.

Huyer, A., R. L. Smith, and B. M. Hickey, Observations of a warm-core eddy off Oregon, January to March 1978, *Deep Sea Res., 31*, 97–117, 1984.

Kolpack, R. L., and D. E. Drake, Transport of clays in the eastern part of Santa Barbara Channel, Calif. *Geo. Mar. Lett., 4*, 191–196, 1985.

Lynn, R. J., and J. J. Simpson, The California Current system; The seasonal variability of its physical characteristics, *J.Geophys. Res., 92*, 12,947–12,966, 1987.

Lynn, R. J., K. A. Bliss, and L. E. Eber, Vertical and horizontal distributions of seasonal mean temperature, salinity, sigma-*t*, stability, dynamic height, oxygen and oxygen saturation in the California Current, 1950–1978, *CalCOFI Atlas 30*, 513 pp., State of Calif. Mar. Res. Comm., La Jolla, 1982.

Montgomery, R. B., A suggested method for representing gradient flow in isentropic surfaces, *Bull. Am. Meteorol. Soc., 18*, 210–212, 1937.

Montgomery, R. B., Transport of the Florida Current off Habana, *J. Mar. Res., 4*, 198–219, 1941.

Montgomery, R. B., and E. D. Stroup, Equatorial waters and currents at 150°W in July–August 1952, *Johns Hopkins Oceanogr. Stud., 1*, 68 pp., 1962.

Munk, W., Internal waves and small-scale processes, in *Evolution of Physical Oceanography*, edited by B. A. Warren and C. Wunsch, pp. 264–291, MIT Press, Cambridge, Mass., 1981.

Owen, R. W., Eddies of the California Current system: Physical and ecological characteristics, in *The California Island: Proceedings of a Multidisciplinary Symposium*, edited by D. Power, 787 pp., Santa Barbara Museum of Natural History, Santa Barbara, Calif., 1980.

Reid, J. L., Jr., Measurements of the California Countercurrent at a depth of 250 m, *J. Mar. Res., 20*, 134–137, 1962.

Reid, J. L., and A. W. Mantyla, The effect of the geostrophic flow upon coastal sea elevations in the northern North Pacific Ocean, *J. Geophys. Res., 81*, 3100–3110, 1976.

Reid, J. L. Jr., G. I. Roden, and J. G. Wyllie, Studies of the California Current system, *CalCOFI Rep., 6*, pp. 27–56, Calif. Coop. Oceanic Fish. Invest., La Jolla, 1958.

Reid, J. L., Jr., E. Coughran, and C. Worral, Detailed measurements of a shallow salinity minimum, *J. Geophys. Res., 69*, 4767–4771, 1964.

Shepard, F. P., and K. O. Emery, Submarine topography off the California coast: Canyons and tectonic interpretations, *Spec. Pap. Geol. Soc. Am., 31*, 171 pp., 1941.

Simpson, J. J., and R. J. Lynn, A mesoscale eddy dipole in the offshore California Current, *J. Geophys. Res.*, this issue.

Simpson, J. J., T. D. Dickey, and C. J. Koblinsky, An offshore eddy in the California Current system, I, Interior dynamics, *Prog. Oceanogr., 13*, 5–49, 1984.

Simpson, J. J., C. J. Koblinsky, J. Peláez, L. R. Haury, and D. Wiesenhahn, Temperature—plant pigment—optical relations in a recurrent offshore mesoscale eddy near Point Conception, California, *J. Geophys. Res., 91*, 12,919–12,936, 1986.

Stommel, H., On the cause of the temperature-salinity curve in the oceans, *Proc. Natl. Acad. Sci., U.S.A., 48*, 764–766, 1962.

Sverdrup, H. U., and R. H. Fleming, The waters off southern California, March to July 1937, *Bull. 4*, pp. 261–378, Scripps Inst. of Oceanogr., Univ. of Calif., La Jolla, 1941.

Swaters, G. E., and L. A. Mysak, Topographically-induced baroclinic eddies near a coastline, with application to the northeast Pacific, *J. Phys. Oceanogr., 15*, 1470–1485, 1985.

Tabata, S., The anticyclonic, baroclinic eddy off Sitka, Alaska, in the northeast Pacific Ocean, *J. Phys. Oceanogr., 12*, 1260–1282, 1982.

Wooster, W. S., and J. H. Jones, California Undercurrent off northern Baja California, *J. Mar. Res., 28*, 235–250, 1970.

R. J. Lynn, Southwest Fisheries Center, National Marine Fisheries Service, National Oceanic and Atmospheric Administration, P. O. Box 271, La Jolla, CA 92038.

J. J. Simpson, Scripps Institution of Oceanography, La Jolla, CA 92093.

(Received May 22, 1989;
accepted August 18, 1989.)